


New stable waterborne amorphous polylactic acid/organoclay nanocomposites prepared using emulsification solvent evaporation method

Chenni Abdenour^{1,2} | Phuong Nguyen-Tri^{1,2}  | Bruno Chabot² |
Simon Barnabé² | Julien Bley³ | Balázs Tolnai⁴ | Njamen Guy⁴ |
Mostafa Eesaee^{1,2}

¹Laboratory of Advanced Materials for Energy and Environment, Université du Québec à Trois-Rivières, Trois-Rivières, Québec, Canada

²Institut d'Innovations en Écomatériaux, Écoproduits et Écoénergies, Université du Québec à Trois-Rivières, Trois-Rivières, Québec, Canada

³Innofibre, Trois-Rivières, Québec, Canada

⁴Kruger Inc., Montréal, Québec, Canada

Correspondence

Phuong Nguyen-Tri, Laboratory of Advanced Materials for Energy and Environment, Université du Québec à Trois-Rivières, 3351, boulevard des Forges, C.P. 500, Local 3170, CIPP, Trois-Rivières, QC G9A 5H7, Canada.

Email: phuong.nguyen-tri@uqtr.ca

Funding information

Natural Sciences and Engineering Research Council of Canada

Abstract

Water based polylactic acid (PLA)-surface modified montmorillonite (MMt) nanocomposites as biobased formulations for paper coating were successfully developed using emulsification solvent evaporation method. Electrostatic and steric stabilization mechanisms have contributed to the production of stable emulsions up to 5 months at $23 \pm 1^\circ\text{C}$, revealing strong repulsive forces generated between the nanoparticles as confirmed by zeta potential (ζ) and dynamic light scattering (DLS) analysis. MMt particles were fully encapsulated by PLA as demonstrated by transmission electron microscopy (TEM) micrographs. Meanwhile the film formation process highlighted the importance of emulsifier's type and solubility in the polymer matrix, as no films were obtained when sodium oleate was used alone compared with continuous, homogeneous, and free-standing films obtained when the combination Tween 80 (80 wt %)—sodium oleate (20 wt%) was used. Scanning electron microscopy (SEM) micrographs of the cross-section's surfaces showed homogeneous dispersion of the MMt particles with no clusters or agglomerates formed. Thermal analyses using differential scanning calorimetry and thermogravimetric analysis (DSC-TGA) showed an overall reduction in the glass transition temperature (T_g) and the thermal stability of neat PLA, however this reduction was recovered when MMt was added due to the confinement effect. Thickened PLA and PLA/MMt emulsions using 1 wt% xanthan gum showed a non-Newtonian behavior and shear thinning flow with suitable viscosity values for paper coating applications.

Highlights

- Development of stable PLA/organoclay nanocomposite aqueous dispersions.
- Steric and electrostatic mechanisms provided excellent stability.
- Full encapsulation of organoclay platelets in nanometric PLA particles.
- Formation of free-standing films from PLA/organoclay emulsions.
- Thickened PLA/organoclay emulsions using Xanthan gum for paper coatings.

KEYWORDS

aqueous media, films, nanocomposites, organoclays, paper coatings, polylactic acid

1 | INTRODUCTION

In recent years, polymer nanocomposites have gained much more interest and emerged as a class of versatile advanced materials. A numerous denomination of applications in coatings and adhesives fields have been unlocked by the advancement in this category of materials.¹ The concept behind creating this category of materials is based on generating a large interface of interactions between the nanometric fillers and polymer chains, the more this interface is large the more likely to produce new materials with new enhanced properties.² The polymer/clay nanocomposites are the new route to prepare end products with improved barrier, thermomechanical performances, chemical resistance, and flame retardation properties, these properties are not to be found in the two components taken separately. Indeed, these properties are strongly dependent on the nanofillers dispersion quality in polymer matrix. Therefore, a good homogenous dispersion at nanometric scale is the main goal during the preparation of these types of materials. However, it is a difficult task to achieve because the nanofillers tend to agglomerate due to the strong van der Waals forces between the particles resulting in macro or micro-composites with poor properties.³ Therefore, surface modification and functionalization of the nanofillers are the most common techniques employed to improve the interfacial interactions and the polymer/nanofillers compatibility and thus to prepare nanocomposites with high performance for advanced applications.^{1,3}

Among different biodegradable polymers used to prepare bio-nanocomposite materials, polylactic acid (PLA) is the most promising biobased polymer as a substitute to the conventional nonbiodegradable polymers. It is a linear thermoplastic polyester produced using ring opening polymerization of L-lactides and D, L-lactides, respectively, cyclic dimers obtained by the depolymerization of the lactic acid, the latter is obtained by fermentation of corn, sugar cane, and so on.⁴ The ratio between the enantiomers L and D is shown to be significantly affecting the properties of the produced PLA, the commercial PLA grades are composed of poly(L-lactide) acid and poly(D, L-lactide) acid. Besides its biodegradability using composting conditions, PLA exhibits interesting mechanical properties comparable to those of polyethylene terephthalate (PET) and polystyrene (PS) with a low T_g compared with both.^{5,6}

On another hand, PLA exhibits low barrier properties to gas, low thermal stability, toughness brittleness, and

low crystallization rates.^{7,8} To overcome these limitations, the dispersions of lamellar nanofillers into PLA matrix proved to have a significant positive effect on its overall performances only when the dispersion is maintained at the nanometric scale instead of micro or macro-metric scale.⁹ Among the nanofillers, layered silicates, such as saponite, mica, hectorite, and so on, are the most used to prepare polymer nanocomposites, but the most widely used clay is montmorillonite having a lamellar structure that belongs to the 2:1 phyllosilicate. With a crystal structure consisting of two layers composed of SiO_4 -tetrahedron and one sandwiched layer composed of Al-octahedron, water molecules are localized between three-layer ions of Al, Fe, and Mg.¹⁰ PLA reinforced with montmorillonite nanocomposites have been extensively reported in the literature.^{11–13}

Besides some enhancement in the thermomechanical properties of the final nanocomposites, the issue of incompatibility between the hydrophobic PLA and the hydrophilic montmorillonite was mostly reported, leading to the formation of micro-composites with poor properties.¹⁴ As an interesting solution the use of organoclays more specifically surface modified montmorillonite (MMt) to prepare PLA nanocomposites have gained much more interest in the last decade, due to the large interface of the organoclay platelets interacting with PLA chains combined with the very high aspect ratio provided by the dispersion at the nanometric scale in form of intercalation, exfoliation, or intercalation/exfoliation structures.¹⁵ Moreover, the presence of the nano-dispersed organoclays in neat PLA matrix significantly improves its gas and water vapor barrier properties by affecting its crystallization rate and creating a tortuous pathway.⁵ There are four main ways to prepare PLA nanocomposites, direct intercalation molten, in situ polymerization, sol-gel process and intercalation by polymer solution.¹⁰ As a form of in situ polymerization method, encapsulating the organoclay in the polymer matrix then dispersion into an aqueous medium, this route has received considerable research interest since not only the ecofriendly nature of these systems but also the variety of applications that uses this type of products, such as paper coating for packaging purposes, waterborne paints, drug delivery systems, adhesives, and so on.⁹ The most widely used processes to produce this type of polymer nanocomposite dispersions is by conventional emulsion polymerization,^{16–18} or by miniemulsion polymerization.^{19,20} Another widely used technique to prepare aqueous polymer dispersions is emulsification solvent evaporation method, which is a two steps technique requiring initially the

emulsification of polymer solution in volatile solvent followed by solvent evaporation resulting in harden polymer particles dispersed in aqueous medium, as reported in the following studies.^{21,22}

Water based, nontoxic, biodegradable with better thermomechanical and barrier properties compared with PLA matrix, this new class of materials with a very interesting and promising properties allows them to be used in a wide range of applications. Hence, their application as a heat sealable barrier coating materials for paper, which constitutes a new research route to prepare a full “green” packaging paper. Our present work subscribes in this optic, and it represents a continuity to our last contribution in this field.²¹ To our best of knowledge water based amorphous PLA-organoclay nanocomposites prepared using as processing method the emulsification-solvent evaporation technique and as components low toxic, food grade and generally safe, has not been reported in the literature making the developed product a novel coatings material with high potential to be applied in the paper packaging field.

2 | EXPERIMENTAL

2.1 | Materials

The biopolymer used in this study is an amorphous PLA purchased from Total-Carbion PLA (Luminy® LX-975), with a melt flow index (MFI) of 10 g/10 min (ISO 1133-A (210°C/2.16 kg)), a density of 1.24 g/cm³ and contains 88% of L-lactide. Two types of emulsifiers with different properties were used. Polysorbate 80 (Tw80) as nonionic emulsifier with hydrophilic lipophilic balance (HLB) value of 15 was supplied by Fisher BioReagents, and sodium oleate (SO) with HLB value of 20 used as anionic emulsifier was supplied from TCI America™.

Surface MMt containing 35–45 wt% of dimethyl dialkyl (C14–C18) amine, with particle size ≤ 20 μm , was used as an organo-modified nanofiller, and was purchased from Sigma-Aldrich. Xanthan gum was used as a thickening agent and was purchased from TCI America™. Ethyl acetate was purchased from Thermo-Fisher Scientific as a low-toxic solvent with 99.5% purity. All the products were used as received without further purification.

2.2 | Preparation procedures

First, PLA solution was prepared by dissolving 6.4 g of PLA granules in 80 mL of ethyl acetate to achieve a concentration of 8 (wt%/vol%), followed by adding different amounts of MMt, 1, 3, and 5 wt% based on the weight of PLA. To better disperse MMt in the PLA solution, the

blend solutions (PLA/1, 3, and 5 wt% MMt) used as the organic phase were vigorously stirred for 5 h followed by ultrasonic bath treatment for 1 h. The second step was the dispersion of the organic phase into the aqueous phase, containing dissolved emulsifiers with various concentrations, and HLB values as presented in Table 1. The selected volume ratio was (O/W) 80/70 vol% to produce emulsions with a theoretical solids content varying from 10.94% to 13.10% depending on the formulation. The dispersion process consisted of a mechanical dispersion at 20,000 rpm for 8 min at room temperature ($23 \pm 1^\circ\text{C}$) using a Dispermat LC-55 dissolver. The resulting emulsions were then classified to stable and unstable by observing the creaming phenomenon after a standing time of 30 min. The selected stable emulsions were then homogenized using an ultrasonic probe (Branson 550 Digital Sonifier) at an amplitude of 40% generating a power of 280 W for 3 min to further decrease the size of PLA droplets and homogenize the emulsions. The final step was the evaporation of ethyl acetate content under slow stirring overnight using a magnetic stirrer at room temperature ($23 \pm 1^\circ\text{C}$), resulting in an aqueous PLA and PLA/MMt nanocomposites suspensions with a milky aspect for emulsion containing only PLA and slowly the color changes gradually becoming slightly opaque by increasing the concentration of MMt. The complete process is presented in Figure 1.

2.2.1 | Film formation

To prepare films from PLA and PLA/MMt emulsions, 20 mL of each emulsion was poured into a glass Petri-dish (diameter 6 cm), the samples were then put in a thermal vacuum oven (Isotemp vacuum oven model 282a) to dry at 120°C for 4 h. The minimal film formation temperature for emulsions prepared based on this grade of PLA was determined in our previous work.²¹

2.2.2 | Emulsion thickening

Thickened emulsions with appropriate viscosity depending on the coating technique are usually used to coat paper due to their processability and good spreading. To adjust the apparent viscosity of the emulsions, xanthan gum was used as a thickening agent. After the complete evaporation of the solvent, 1 wt% of xanthan gum was added to increase the apparent viscosity of the prepared emulsions and thus allow to prepare suitable thickened emulsions with high apparent viscosity 500–1000 mPa·s for laboratory bar coating applications as recently reported.²¹ Vacuum mixing was used at 1200 rpm for 2 h at room temperature ($23 \pm 1^\circ\text{C}$)

Formulations	MMt (wt%) ^a	Organic phase	
		Ethyl acetate (mL)	Concentration (wt%/vol%)
PLA	0	80	8
PLA/MMt 1%	1		8.08
PLA/MMt 3%	3		8.24
PLA/MMt 5%	5		8.40

Emulsifiers	HLB values ^b	Aqueous phase	
		Concentration (wt%)	Water (mL)
Tw80	15	0.5–1.8–3.5	70
SO	20	0.5–1.8–3.5	
SO-Tw80 (20:80)	16	0.5–1.8–3.5	

TABLE 1 Formulations used to prepare poly(lactic acid) (PLA)/modified montmorillonite (MMt) emulsions.

^aSurface modified montmorillonite.

^bHydrophile lipophile balance.

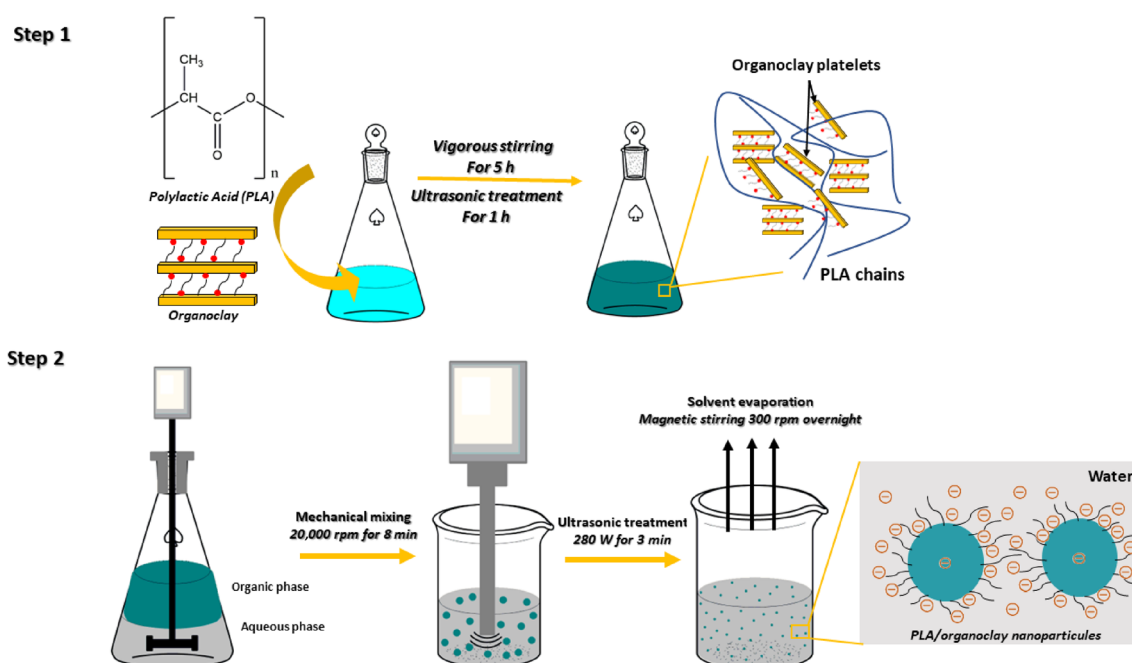


FIGURE 1 Experimental process for the preparation of PLA/SM-Mt aqueous emulsions. PLA, poly(lactic acid).

to provide a good dissolution of xanthan gum and to avoid the production of air bubbles.

3 | CHARACTERIZATION METHODS

3.1 | Solid content, particle size, and zeta potential (ζ)

The solid contents of the prepared stable emulsions were measured according to ISO 1625 standard method. A volume of PLA and PLA/MMt emulsions was dried to

constant mass at 125°C to determine the solids concentration. The proportion of dried matter to the total mass of the sample was used to calculate the solid content. The particle size of PLA and PLA/MMt nanocomposites were measured using the DLS method operating on a Zeta-sizer “Malvern model Zen 3600” instrument, which measures first the Brownian motion of the particles in a sample and then calculates their size from the established theories. Before being transferred to the sample cell, the emulsions were diluted with deionized water for the determination of the polydispersity index (PDI) and the mean particle size distribution, measurements were conducted in three replicates.

To measure the zeta potential of PLA and PLA/MMT particles, analyses were conducted on a zeta-sizer (Model Zen 3600; Malvern Instruments Ltd., Malvern Worcestershire, UK), which works using a combination of the measurement techniques: electrophoresis and laser doppler velocimetry. Before testing, samples were diluted in distilled water for zeta potential measurement in three replicates.

The kinetic stability of the prepared emulsions was assessed in two stages process. First stage consists of visual observations, the phase separation after a standing time of 30 min following the production process and after the complete evaporation of the solvent ethyl acetate. This method helped us to select and identify emulsions showing preliminary stability based on the type of the used emulsifiers and their concentrations. The second stage consists of storing the emulsions that showed stability for more than 24 h, by transferring a volume of 50 mL of each emulsion into a transparent glass container at room temperature ($23 \pm 1^\circ\text{C}$). Phase separation by sedimentation and coalescence was assessed. This stage is very important for emphasizing the effect of emulsifier's type and concentrations on the stability of the prepared emulsions.

3.2 | Thermal analysis (DSC-TGA)

The DSC analysis was conducted to evaluate the T_g of PLA/MMT nanocomposites compared with neat PLA granules. Samples were cut into small pieces weighing between 10 and 30 mg. The analysis was conducted on DSC apparatus "TA Instruments the Discovery DSC2500." First, the sample was heated from -10 to 220°C at a rate of $10^\circ\text{C}/\text{min}$, as a first heating run to remove its thermal history, followed by cooling to -10°C at a cooling rate of $10^\circ\text{C}/\text{min}$. The T_g of the samples was defined by a second heating run from -10 to 220°C at a heating rate of $10^\circ\text{C}/\text{min}$.

Thermal stability of the developed films was studied using TGA analysis by comparing thermal stability of PLA neat and its composite. First, composite samples were cut into small pieces weighing from 25 to 35 mg, then placed in a ceramic plate. The data of the thermal stability was recorded by heating the samples from 40 to 800°C , using "PerkinElmer Thermal Analysis" at heating rate of $10^\circ\text{C}/\text{min}$, in air atmosphere.

3.3 | Morphology analyses

A scanning electron microscope (SEM-Hitachi VP-SEM SU1510) was used to analyze the morphologies of PLA and PLA nanocomposite films. Samples were gold-coated by sputtering and the measurements were then taken at a

10 kV accelerating voltage. The elemental composition analysis of the samples was carried out by means of the energy dispersive x-ray (EDX) analysis using an energy dispersive spectrometer Oxford X-max 20 mm^2 coupled to the SEM-Hitachi VP-SEM SU1510, at a 15 kV accelerating voltage. The morphology of the particles and the dispersion of MMT in PLA matrix were investigated using TEM analysis. First, 10 mL from emulsions prepared using only Tw80 and emulsions prepared using 3.5 wt% of SO + Tw80 (20:80) were poured into glass Petri dishes and placed in laboratory fume hood at room temperature $23 \pm 1^\circ\text{C}$ for 72 h to dry, finally the samples were recovered in form of powders. To prepare the nanoclay sample, 5 mg of MMT was diluted in ethanol since it is hydrophobic compound and cannot properly be dispersed in distilled water. The emulsion's powders were gently ground then dispersed in a volume of distilled water to form diluted suspensions. Before analysis, few droplets of each sample were poured on to a 300 mesh copper grids, then the water content was dried out. The analyses were carried out on a transmission electron microscope (TEM) Philips EM208S at 80 kV accelerating voltage.

3.4 | Rheology behavior

The rheological behavior was studied by measuring the viscosity (η), shear rate ($\dot{\gamma}$), and shear stress (τ) of aqueous emulsions and the thickened emulsions using xanthan gum (1 wt%) prepared using SO-Tw80 (20:80) at 3.5 wt%. The choice of these formulations was based promising results previously obtained and expected viscosities required for coating paper applications. The measurements were conducted on a rheometer (Rheologica Stressch), the viscosity of the samples was measured using a concentric cylinder cup and constant rate method at room temperature $23 \pm 1^\circ\text{C}$. This method measures viscosity and stress as a function of shear rate, useful for simulating specific steps of a process like paper coating. Precisely, 15.9 mL of each sample were poured into the interior of the cylindrical cup, then the rotor was automatically submerged into the sample until the point zero was setup. The shear rate $\dot{\gamma}$ ($1/\text{s}$) was varied from 10^{-6} to 631 s^{-1} and the measurements were replicated three times.

4 | RESULTS AND DISCUSSIONS

4.1 | Particle size distribution and zeta-potential (ζ)

Particle size and surface charge are the most studied factors to assess the extent of the physical stability of an

emulsion.²³ Oil-in-water emulsions are thermodynamically unstable systems composed of two immiscible phases with different viscosities. Two common types exist: the conventional emulsions having droplets size larger than 100 nm and the nano-emulsions with an average particle size $d < 100$ nm.²⁴ The smaller the size of the droplets, the more stable emulsions will be. This is due to the Brownian motion overcoming gravity, which prevents their coalescence by preventing surface flocculation and therefore no coagulation and aggregation will occur.²⁵ DLS was used to determine the average particle size and the PDI of the prepared emulsions. As we can observe from the results reported in Table 2, conventional emulsions were obtained with an average particle size in the range of 145–352 nm, with PDI values in the range of 0.1–0.3, corresponding to a relatively homogeneous dispersion. It is well established that the PDI values are a good indicator of the homogeneity of the particle size distribution which is the most important parameter affecting the fundamental properties of emulsions.²⁶

The incorporation of MMT has led to an increase in PLA's particle size, varying from 7 to 140 nm increase depending on the concentration of the incorporated clay, the type of the surfactants and their concentrations, as we can observe in Table 2. A slight increase in PDI values of PLA/MMt emulsions was observed, since the presence of MMT in PLA particles altered the homogeneity of the

particle size distribution as shown in the TEM micrographs (Figure 2). Surface MMT has a lamellar structure as we can see in Figure 2A. From Figure 2B,C, we can see that PLA particles without the addition of MMT has a homogeneous spherical form compared with PLA particles containing 1, 3, and 5 wt% of MMT where irregularities and uneven forms are visible as shown in Figure 2D–F. These results agree with those reported in the literature.²⁷

On another hand, from Table 2 and as confirmed by TEM micrograph in Figure 2B, formulations prepared with only Tw80 have the largest particle size and the highest PDI value, which explains the instability and the sedimentation that occurred after a short storage time.²⁸

Another important surface characteristic is the surface charge. The zeta potential (ζ) provides important information about the surface charge of the particles in the sliding plane, which significantly influences the stability of colloids. At a high zeta potential absolute value, there is a low susceptibility for the suspended polymer particles to coagulate due to the electrostatic repulsive forces.²⁹ Particles with zeta potential values outside the interval $[-30, +30]$ mV generates high electrostatic repulsive forces, which prevent their collision and coagulation.³⁰

The measured ζ -potential values are summarized in Table 2. As observed, emulsion prepared using only Tw80 has a ζ -potential value of -26 mV, which are

TABLE 2 Different properties of polylactic acid (PLA) and PLA/modified montmorillonite (MMt) emulsions.

Formulations	Surfactant type	HLB	Concentration (wt%) ^a	Particle size (nm)	PDI ^b	ζ -potential (mV)	Solids content (%)
PLA	Tw80	15	3.5	2230	0.76	-26	11.85
PLA	SO	20	1.8	172	0.20	-51	9.25
PLA/MMt 1%	SO	20	1.8	183	0.23	-48	10.45
PLA/MMt 3%	SO	20	1.8	194	0.25	-41	11.12
PLA/MMt 5%	SO	20	1.8	201	0.30	-36	11.30
PLA	SO	20	3.5	146	0.19	-61	12.00
PLA/MMt 1%	SO	20	3.5	156	0.22	-58	12.15
PLA/MMt 3%	SO	20	3.5	165	0.27	-51	12.65
PLA/MMt 5%	SO	20	3.5	182	0.24	-47	13.00
PLA	SO + Tw80 (20:80)	16	1.8	189	0.10	-43	9.00
PLA/MMt 1%	SO + Tw80 (20:80)	16	1.8	193	0.15	-38	10.05
PLA/MMt 3%	SO + Tw80 (20:80)	16	1.8	208	0.18	-35	10.88
PLA/MMt 5%	SO + Tw80 (20:80)	16	1.8	210	0.24	-32	11.00
PLA	SO + Tw80 (20:80)	16	3.5	175	0.17	-53	11.85
PLA/MMt 1%	SO + Tw80 (20:80)	16	3.5	168	0.13	-49	12.00
PLA/MMt 3%	SO + Tw80 (20:80)	16	3.5	182	0.14	-46	12.35
PLA/MMt 5%	SO + Tw80 (20:80)	16	3.5	195	0.18	-44	12.80

^aWeight concentration.

^bPolydispersity index.

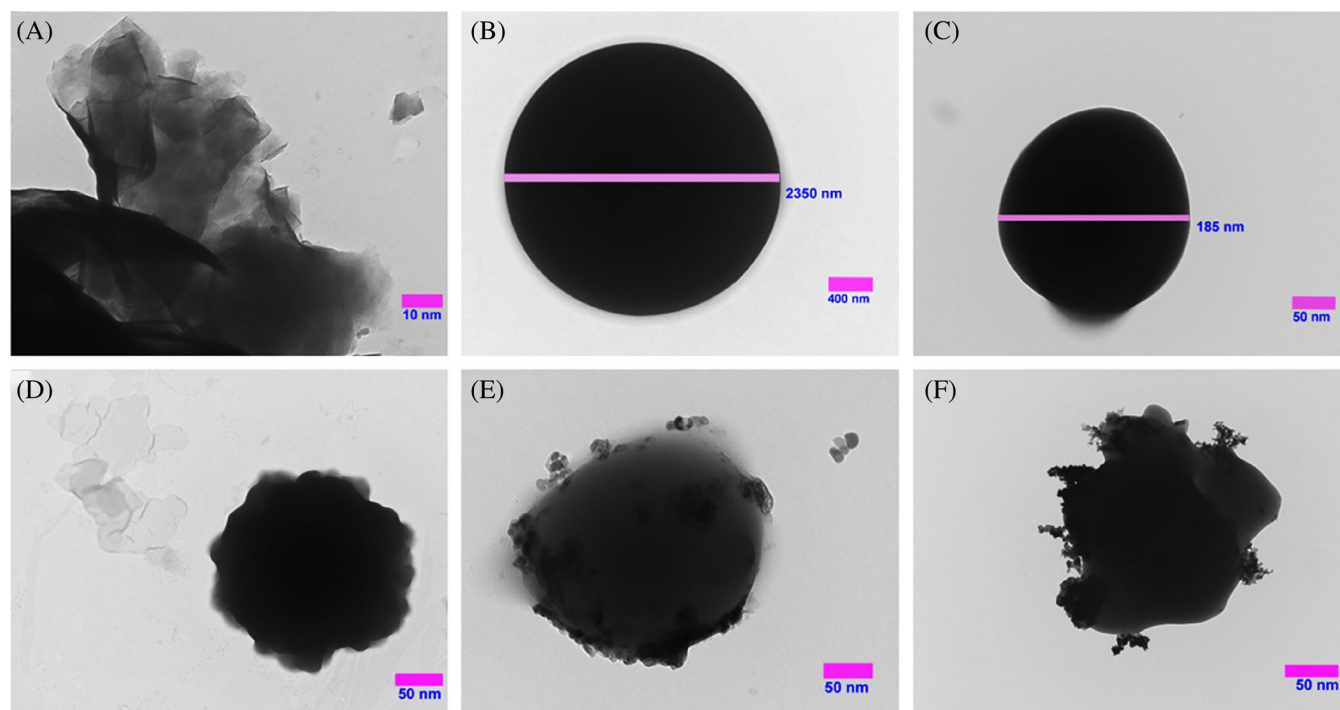


FIGURE 2 Transmission electron micrographs of (A) modified montmorillonite (MMt), (B) polylactic acid (PLA) particle prepared using Tw80, (C) PLA particle prepared using 3.5 wt% of SO + Tw80 (20:80), (D) PLA-1 wt% MMT, (E) PLA-3 wt% MMT, and (F) PLA-5 wt% MMT emulsion prepared using 3.5 wt% of SO + Tw80 (20:80).

within the interval previously defined. Therefore, weak electrostatic repulsive forces between such particles are not sufficient to prevent flocculation and coalescence. This was expected since Tw80 is a nonionic small molecule surfactant adsorbed on the surface of the particles. It maintains emulsion's stability due to the steric stabilization mechanism. The negative ζ -potential recorded for this formulation is attributed to the carboxylic acid groups of PLA oriented toward the particle surface due to the polar interactions with the aqueous medium, followed by an equilibrium between the acid and its conjugate base, creating the negative charges on the surface of the particles.³¹

However, when anionic emulsifier was used, the ζ -potential values were significantly decreased reaching -61 mV when SO was used alone at a concentration of 3.5 wt% and -53 mV with only 20 wt%. Therefore, these conditions generated a strong electrostatic stability. By adding MMT, a slight increase in the ζ -potential values was noticed and this can be explained by the self-arrangement of MMT within the PLA particles. TEM micrographs in Figure 2C–E revealed that MMT layered silicate were both encapsulated and dispersed on the surface of PLA particles. This was expected since MMT is an organically modified clay, and it is compatible with the organic phase (PLA solution). Moreover, the presence of MMT layers on the surface of PLA particles most likely

hindered the surface charge distribution by reducing the number of emulsifiers present on the surface and thus the ζ -potential values.³² On another hand, adding hydrophilic clay like natural montmorillonite has a different effect on zeta potential and stability of the prepared emulsions. The addition of Na-montmorillonite to polystyrene latex decreased the ζ -potential values and contributed to prepare a stable pickering emulsion based on polystyrene containing Na-montmorillonite.³³

Generally, a linear correlation between the evolution of ζ -potential and the particle size is observed (Figure 3). Small particle size coincides with higher zeta potential values. This is expected since small size particles provide the higher surface area, which enables more surfactants molecules adsorption and therefore the surface charge increases.

Additional data on the stability assessment are necessary to better understand the initial selection of emulsions based on their gravitational stability. For this purpose, the creaming phenomenon as a good indicator of instability was observed after 30 min of completing the emulsification process. Systems that were completely unstable showed a clear phase separation for a standing time inferior to 30 min and were discarded. Results are presented in Table 3. Two distinct phenomena were obtained depending on different factors like the composition of formulations, emulsifiers type, and concentrations. Emulsions containing

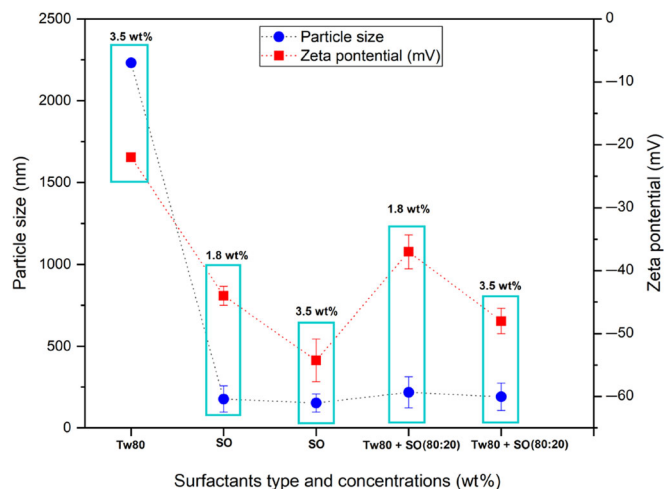


FIGURE 3 Particle size (nm) and zeta potential (mV) variation as a function of surfactants type and concentrations.

only PLA showed a different response compared with those containing the MMT. For emulsions containing only PLA, at lower concentrations of only Tw80 (0.5 and 1.8 wt%) and after finishing dispersion and homogenization, instant instability by creaming and phase separation was observed. However, at a higher concentration, emulsions were formed as shown in Figure 4A. This can be attributed to a very important parameter related to the concentration of the surfactant, which is the total coverage of the droplet's surface,³⁴ in our case no creaming was observed when 3.5 wt% of Tw80 was used. However, it is important to mention that sedimentation occurred after only 72 h of storage at room temperature $23 \pm 1^\circ\text{C}$. The large amount of the organic phase used to prepare the emulsions combined with the low emulsification efficiency of Tw80 may contribute to the fast coagulation rate and thus promoted the formation of large-size PLA particles. These results are different from those obtained in our previous work,²¹ using small amounts of PLA solution, in which the use of a low concentration of nonionic surfactants provided 28 days stability under the same storage conditions.

On another hand, instant phase separation with the formation of a thick layer was observed in the case of PLA/MMt emulsions prepared using only Tw80 at all concentrations (Figure 4A). These results are due to the creaming phenomena occurring when the density of the dispersed phase is lower than that of the continuous phase leading to the rise of the dispersed droplets and forming a thick layer on the top of the aqueous phase after the droplets coalesce.³⁵ The creaming process is reversible, and the two phases of the emulsions can be redispersed by agitation. However, it will harm the stability of the emulsions by causing coalescence, which is an irreversible process.³⁶ Moreover, using Tw80 as an

emulsifier even at high concentrations has not prevented the creaming and the cracking of PLA/MMt emulsions. Tw80 is a low molecular weight ester ~ 1310 g/mol, synthesized from a combination of sorbitan monooleate and ethoxylate.³⁷ As a nonionic emulsifier, it provides stability to the emulsions by creating steric repulsion and thus it hinders the coalescence and aggregation of the dispersed droplets. To achieve this efficiency, the emulsifier molecules must cover entirely the oil/water interface.³⁸ However, due to the low molecular weight of Tw80, the mobility of its molecules in and out of the oil/water interface creates uncovered surfaces leading to oil droplets' surface exposure and hence the droplets merging forming an oil layer at the top of the emulsions. Furthermore, the presence of the hydrophobic organoclay encapsulated and adsorbed at the surface of PLA droplets can cause problems in controlling droplet size and the coagulation of the emulsions by hindering the complete adsorption of Tw80 molecules. Many studies that used the conventional emulsion polymerization process or mini-emulsion polymerization to prepare nanocomposites emulsions using various organoclay types have reported difficulties to prepare stable latexes and it requires the use of very high amounts of surfactants with high HLB values to reach stability.^{9,39}

The use of an anionic emulsifier (SO) alone or in combination with the nonionic emulsifier (polysorbate 80) led to the formation of stable emulsions for more than 5 months stored at room temperature $23 \pm 1^\circ\text{C}$, except at the very low concentration (0.5 wt%) where coagulation and aggregate formation was observed after the complete solvent evaporation as presented in Figure 4B this result can be explained by the low amount of emulsifier's molecules used and therefore its insufficiency to cover completely the surface of PLA droplets and thus did not prevent surface flocculation and coalescence. Also, it is well known that ionic emulsifiers provide electrostatic stability to polymeric emulsions through electrostatic stability arising from a balance between repulsive and attractive forces creating a potential energy barrier force preventing polymer particles from approaching and colliding and finally coagulating. Therefore, coagulation observed at low concentrations can be due to the attraction forces mainly van der Waals forces between polymer particles overcoming the repulsive forces generated by the anionic emulsifier.⁴⁰ No coagulation was observed at concentrations above 0.5 wt% indicating that the energy barrier resulting from the electrostatic combined with steric forces was higher than the van der Waals attractive forces which mostly prevented particles from coagulating. Many studies have reported the preparation of stable polymer/clay nanocomposites latexes using large amounts of anionic emulsifier like sodium dodecyl sulfate (SDS) up to 8 wt%.⁴¹

TABLE 3 Summary of all visual observations.

Formulations	MMt (wt%) ^a	Emulsifiers type	Emulsifier's concentration (wt%)	Dispersion stability
PLA	0	Tw80 ^b	0.5	Creaming
PLA/MMt 1% ^c	1	Tw80	0.5	Creaming
PLA/MMt 3%	3	Tw80	0.5	Creaming
PLA/MMt 5%	5	Tw80	0.5	Creaming
PLA	0	Tw80	1.8	Creaming
PLA/MMt 1%	1	Tw80	1.8	Creaming
PLA/MMt 3%	3	Tw80	1.8	Creaming
PLA/MMt 5%	5	Tw80	1.8	Creaming
PLA	0	Tw80	3.5	Stable
PLA/MMt 1%	1	Tw80	3.5	Creaming
PLA/MMt 3%	3	Tw80	3.5	Creaming
PLA/MMt 5%	5	Tw80	3.5	Creaming
PLA	0	SO ^d	0.5	Coagulation
PLA/MMt 1%	1	SO	0.5	Coagulation
PLA/MMt 3%	3	SO	0.5	Coagulation
PLA/MMt 5%	5	SO	0.5	Coagulation
PLA	0	SO	1.8	Stable
PLA/MMt 1%	1	SO	1.8	Stable
PLA/MMt 3%	3	SO	1.8	Stable
PLA/MMt 5%	5	SO	1.8	Stable
PLA	0	SO	3.5	Stable
PLA/MMt 1%	1	SO	3.5	Stable
PLA/MMt 3%	3	SO	3.5	Stable
PLA/MMt 5%	5	SO	3.5	Stable
PLA	0	SO + Tw80 (20:80)	0.5	Coagulation
PLA/MMt 1%	1	SO + Tw80 (20:80)	0.5	Coagulation
PLA/MMt 3%	3	SO + Tw80 (20:80)	0.5	Coagulation
PLA/MMt 5%	5	SO + Tw80 (20:80)	0.5	Coagulation
PLA	0	SO + Tw80 (20:80)	1.8	Stable
PLA/MMt 1%	1	SO + Tw80 (20:80)	1.8	Stable
PLA/MMt 3%	3	SO + Tw80 (20:80)	1.8	Stable
PLA/MMt 5%	5	SO + Tw80 (20:80)	1.8	Stable
PLA	0	SO + Tw80 (20:80)	3.5	Stable
PLA/MMt 1%	1	SO + Tw80 (20:80)	3.5	Stable
PLA/MMt 3%	3	SO + Tw80 (20:80)	3.5	Stable
PLA/MMt 5%	5	SO + Tw80 (20:80)	3.5	Stable

^aSurface modified montmorillonite.^bTween 80.^cPoly(lactic acid/surface modified montmorillonite (1, 3, and 5 wt%).^dSodium oleate.

Overall, stable PLA emulsions for more than 5 months containing surface MMt at different weight ratios (1, 3, and 5 wt%), were successfully prepared using

simple emulsion solvent evaporation method. The key factor in the preparation of this kind of emulsions with high solids content up to 13% is the use of anionic

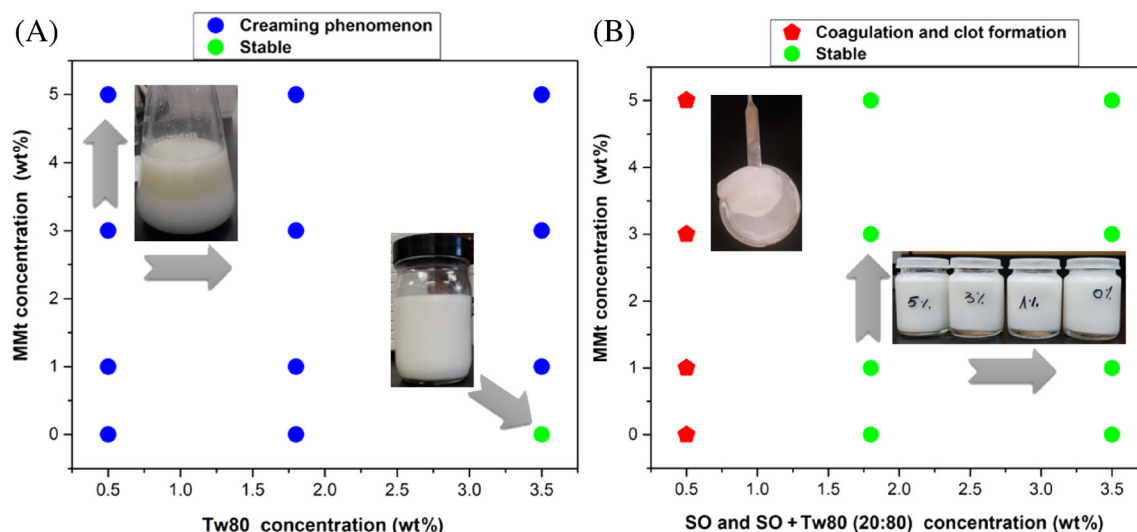


FIGURE 4 Visual observations of the gravitational instability of PLA/MMt emulsions using (A) Tw80, (B) SO, and SO + Tw80 (20:80). MMt, modified montmorillonite; PLA, polylactic acid.

emulsifier (SO) alone or in combination with nonionic emulsifier (Tween80) resulting from the steric and the electrostatic stabilization mechanisms. On the other hand, the use of only Tw80 showed no interesting results especially when surface MMt was added indicating that steric stabilization provided by Tw80 with HLB value of 15 was not sufficient to prepare this kind of emulsions.

4.2 | Film formation, morphology, and thermal properties

The obtained results are shown in Figure 5. As we can observe in Figure 5A–A₃, no films were obtained using only SO as an emulsifier at all concentrations, the results showed fragmented discontinuous and wax-like materials. This can be attributed to the formation of biphasic domains in the polymeric matrix due to the incompatibility of SO and PLA resulting in incomplete coalescence even after 5 h of the drying process.

The distribution of the surfactants used to stabilize the emulsions is usually not homogenous and tend to migrate to the interfaces air–film and substrate–film by forming layers on the top or biphasic domains within the polymeric matrix which represents a serious challenge, since the behavior of the emulsifiers during the coalescence process can alter the final properties of the prepared films.⁴² Which is demonstrated clearly in the obtained results, the behavior of SO and Tw80 was significantly different. In addition to the behavior, another important factor which need to be considered is the solubility of the emulsifiers in the polymer, more precisely the interdiffusion of these low molecular weight substances into a polymeric matrix, if

the emulsifier has a high solubility with the polymer or used in low concentrations, it will facilitate the coalescence of the polymer particles due to its plasticizing effect and therefore a homogenous film will be formed.⁴³

Therefore, emulsifier's solubility in the polymer is a crucial factor affecting the continuity and the homogeneity of the prepared films by affecting the degree of coalescence, low coalescence degree creates discontinuous, nonhomogeneous films.³⁰ On other hand, films were obtained in the case of samples prepared using only Tw80 or the mixture of SO and Tw80 (20:80) as we can observe in Figure 5B–B₃,C. It is suggested that Tw80 due to its high solubility and compatibility with PLA lead to a high coalescence degree and therefore homogeneous and continuous films were formed. PLA films shown in Figure 5B,C were translucent. This result was not expected since the PLA used is amorphous. This can be attributed to the formation of thin layers on both sides of the film surfaces composed of the emulsifiers. Transparent films were obtained when small amounts of Tw80 were used.²¹ Same observation for the formed films containing MMt presented in Figure 5B₁–B₃ opaque, homogenous, and continuous films were formed and the degree of opacity increases by increasing MMt content.

This part of our work is very important, since our goal is the application of the developed emulsions as paper coating formulations. The film formation process is similar to coating paper process where the drying part takes place after the coating and the goal at the end is the formation of a polymeric film recovering the microporous surface of the paper and thus modifying some properties of the paper like reducing its hydrophilicity and its high permeability. Results showed that emulsions prepared

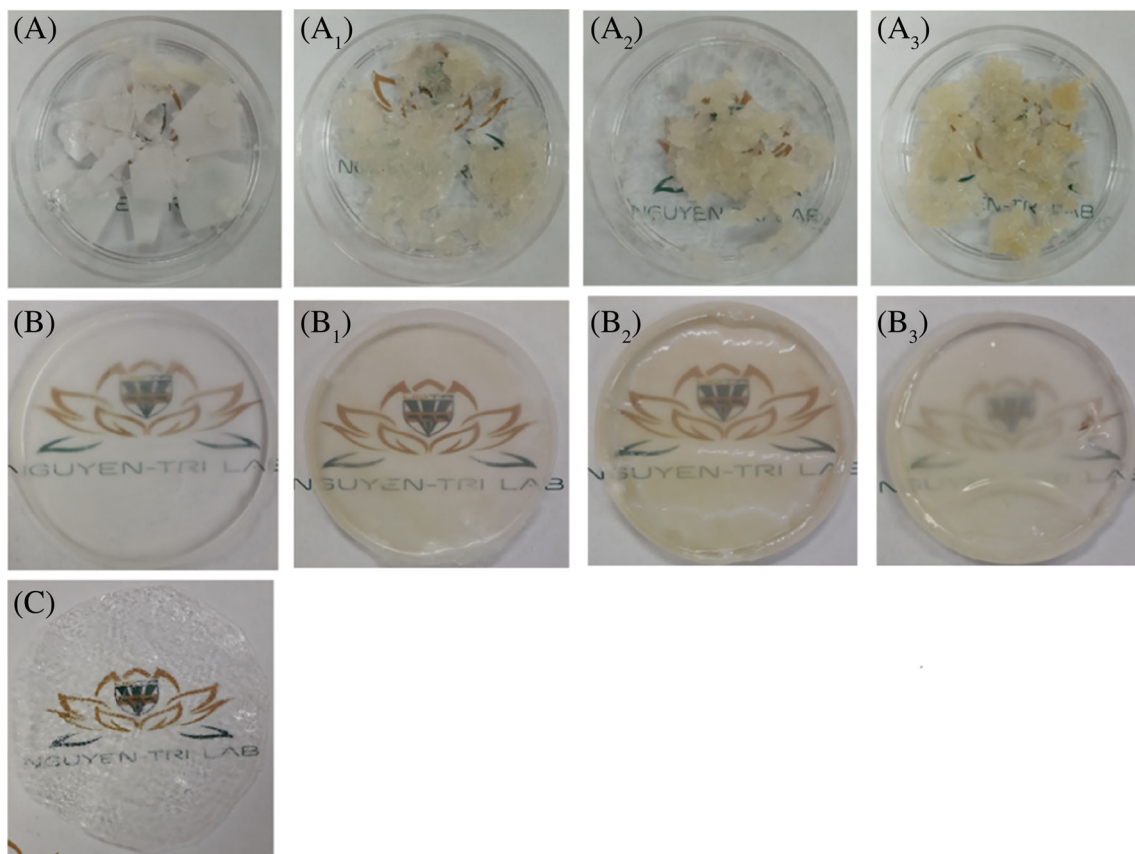


FIGURE 5 Samples obtained after the drying process, using only SO as emulsifier (A) polylactic acid (PLA), (A₁) PLA-1 wt% modified montmorillonite (MMt), (A₂) PLA-3 wt% MMt, (A₃) PLA-5 wt% MMt. Using SO + Tw80 (20:80) as emulsifiers (B) PLA, (B₁) PLA-1 wt% MMt, (B₂) PLA-3 wt% MMt, (B₃) PLA-5 wt% MMt and using only Tw80 (C) PLA.

with only SO were not suitable for paper coating since there was no film formed for all formulations and at all concentrations. Similar results were obtained for the sample prepared using only Tw80 due to the lack of stability showed during storage. Films prepared with the mixture of SO + Tw80 (20:80) will be further investigated since they provided interesting results.

The morphology studies of the prepared films were conducted using SEM coupled with EDX analyses, micrographs of the surfaces. The cross sections and EDX spectra are presented in Figures 6 and 7. First the morphology of the surface MMt was analyzed. As we can observe in Figure 6A, the micrograph shows many crumpled individual small flakes and expanded surface attributed to the chemical intercalation using dimethyl dialkyl amine. The expansion property of the organo-modified clays allowed it to be used in organic compounds adsorption,⁴⁴ improved its swellability in organic solvents⁴⁵ and showed a good compatibility with polymers compared with unmodified natural clays, due to the strong interfacial interactions between montmorillonite and polymers. This enhances significantly the thermomechanical and barrier properties of the final nanocomposites.^{46,47}

To investigate the surface morphology of the prepared films, SEM analysis was conducted. It is important to emphasize that films with homogeneous and cohesive surfaces without cracks, pores, and irregularities provide a major positive effect on mechanical and barrier properties of the coated paper. The SEM micrographs of the surfaces of all films are presented in Figure 6B–E. PLA surface showed a smooth and continuous surface (see Figure 6B), whoever this surface becomes more rougher when MMt is introduced, which is attributed to the distribution of some large MMt tactoids on the surface of the films⁴⁸ and this presence increases by increasing MMt concentration up to 5 wt% as demonstrated in Figure 6C–E. The surface element composition EDX results are presented in Figure 7. From the EDX spectrum of MMt Figure 7A₁ we can observe the presence of mainly four elements, carbon (C), oxygen (O), aluminum (Al), silicon (Si) and traces of magnesium (Mg), iron (Fe), chloride (Cl), and calcium (Ca). The presence of carbon is related to the organic cationic surfactant dimethyl dialkyl amine since the MMt contains 35–45 wt% of the surfactant. The residual elements are the components of the montmorillonite, one unit of montmorillonite is composed of two tetrahedral sheets of silica

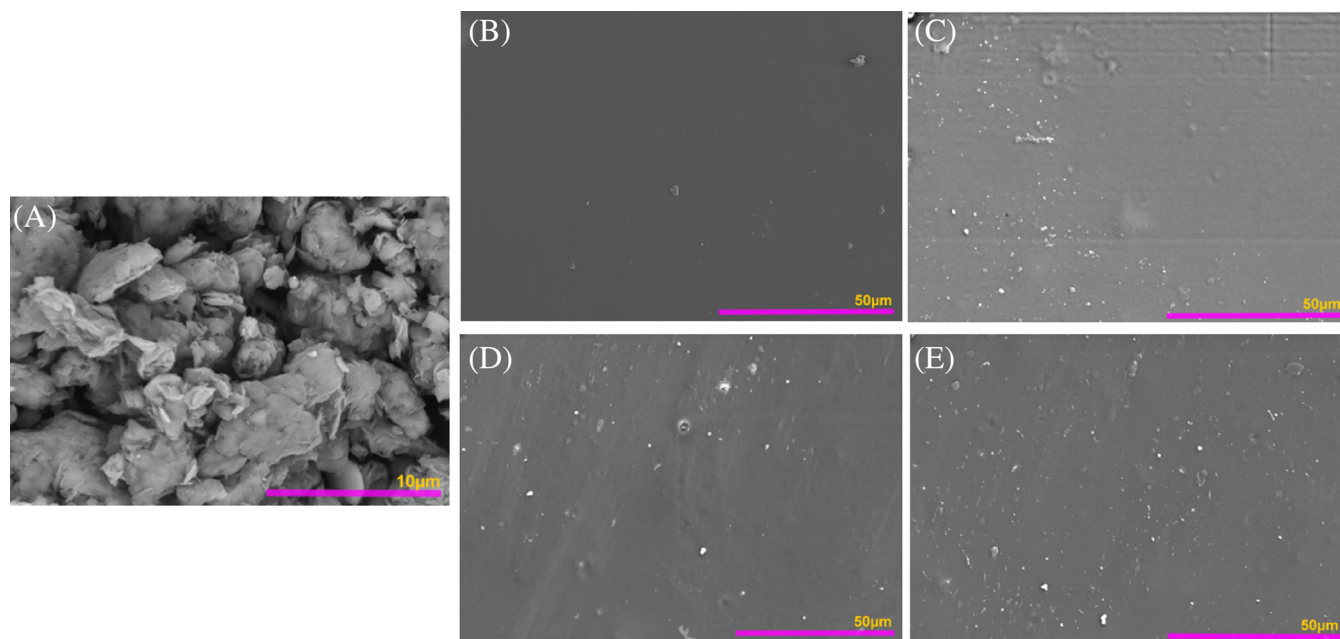


FIGURE 6 Scanning electron microscopy surface microstructure of (A) modified montmorillonite (MMt) powder, (B) PLA film, (C) PLA-1% MMt film, (D) PLA-3% MMt film, and (E) PLA-5% MMt film.

(O—Si—O) and one octahedral of alumina (O—Al(Mg)—O).⁴⁹ Figure 7B–E shows the cross sections micrographs of PLA and PLA containing 1, 3, and 5 wt% of MMt. Figure 7B shows the cross section of PLA film. A continuous and relatively smooth surface related to the well assimilated PLA chains is observed, which demonstrate the effectiveness of the drying process in producing a homogeneous and continuous films.^{8,50} However, in the case of PLA/MMt (1, 3, and 5 wt%) nanocomposites morphological changes attributed to the randomly dispersed MMt particles are noticed, which generated rougher surfaces as the weight ratio of the nanofiller increased as shown in Figure 7D,E. The presence of some compact structures was also observed as aggregates inducing irregularities in the matrix. These results can be attributed to the weak interfacial adhesion between PLA matrix and the MMt particles. Moreover, the expansion ability and the intercalary degree of the organoclay combined with the preparation method are the main factors affecting the uniformity of its dispersion leading to an intercalated or exfoliated structures.^{51,52}

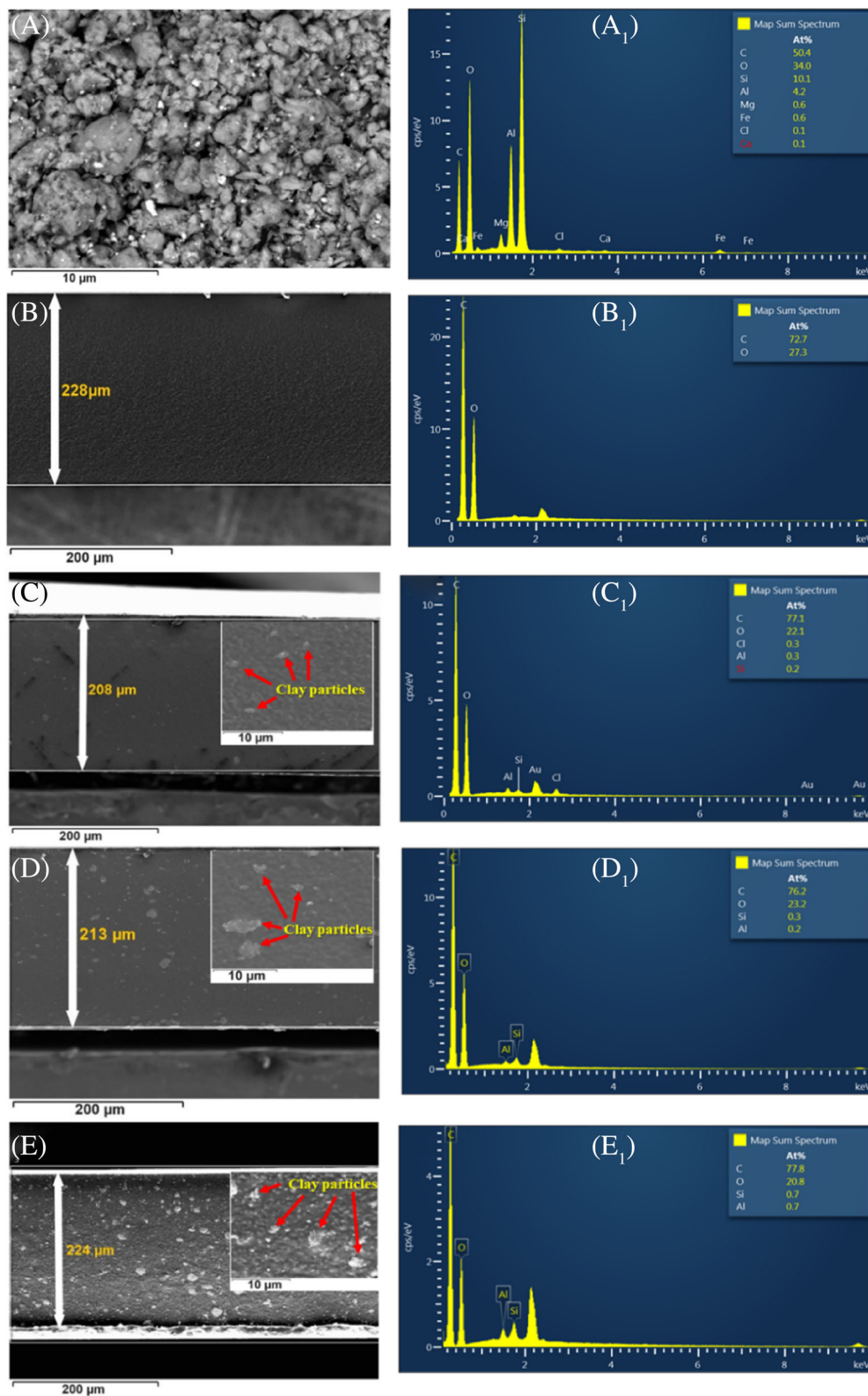
DSC results obtained during the second heating run are presented in Figure 8A. All tested samples exhibited no melt pics during the heating run or crystallization phenomena during the cooling run. This can be attributed to the glassy amorphous structure of the samples implying that the structure of neat PLA remained amorphous. Meanwhile, the T_g of neat PLA granules without any treatment measured at 55.18°C had undergone a major decrease in the case of PLA films prepared from

the aqueous emulsion, the reduction was about 5°C presenting an endothermic pic at 50.53°C as shown in Figure 8B. This decrease in T_g is due to the plasticization effect induced by the emulsifiers. It is well established that T_g is much sensitive to the mobility of the polymer chains and to their local environment.⁵³ Whereas, by adding amounts of MMt the reduction in T_g was slightly recovered ($\sim 6^\circ\text{C}$) up to 56.25°C higher than the T_g of neat PLA granules, this increase can be attributed to the restriction in the polymer's chains movement at the vicinity of the organoclay pallets as a consequence of bonding or adsorbing at the surface of the organoclay.⁵³

Negrete-Herrera et al.⁵³ reported in their study the effect of laponite as nonofiler on the thermal properties of latex films based on poly (styrene-co-n-butyl acrylate). The thermal analysis by DSC showed an increase in the T_g of the nanocomposites up to 12°C compared with the unfilled latex. Also, Ozkoc and Kemalglu⁵⁴ have reported the effect of organoclay (Cloisite 30B) added with different amounts (0–5 wt%) to a plasticized PLA membrane. DSC results showed a decrease in the T_g of the plasticized PLA compared with the neat PLA, when Cloisite 30B was added a slight recovery in T_g of PLA nanocomposites of about 4°C was recorded.

The thermogravimetric analysis results are shown in Figure 8C, the weight loss (%) of all samples is presented in a comparative TGA thermograms, all samples showed one stage thermal degradation, divided in two principal areas: the first area, consists of small weight loss <10% was recorded between 40 and 150°C related to losing

FIGURE 7 Micrographs of (A) modified montmorillonite (MMt) surface, surface of the cross-sections of (B) polylactic acid (PLA) film, (C) PLA-1 wt% MMt film, (D) PLA-3 wt% MMt film and (E) PLA-5 wt% MMt film. Energy dispersive x-ray spectra of (A₁) MMt, (B₁) PLA film, (C₁) PLA-1 wt% MMt film, (D₁) PLA-3 wt% MMt film, and (E₁) PLA-5 wt% MMt film.



weakly and strongly bound water by evaporation, for neat PLA pellets it was only 2% since the sample was dried before analysis, for the rest of samples the water content was higher about 8%–9% this was expected since the films were prepared from aqueous emulsions. PLA is

well known for its low thermal stability demonstrating a rapid loss of molecular weight when exposed to overheating treatment,⁵⁵ the thermal degradation of PLA depends on various factors like residence time, temperature, moisture and catalyst presence, chemical structure, molecular

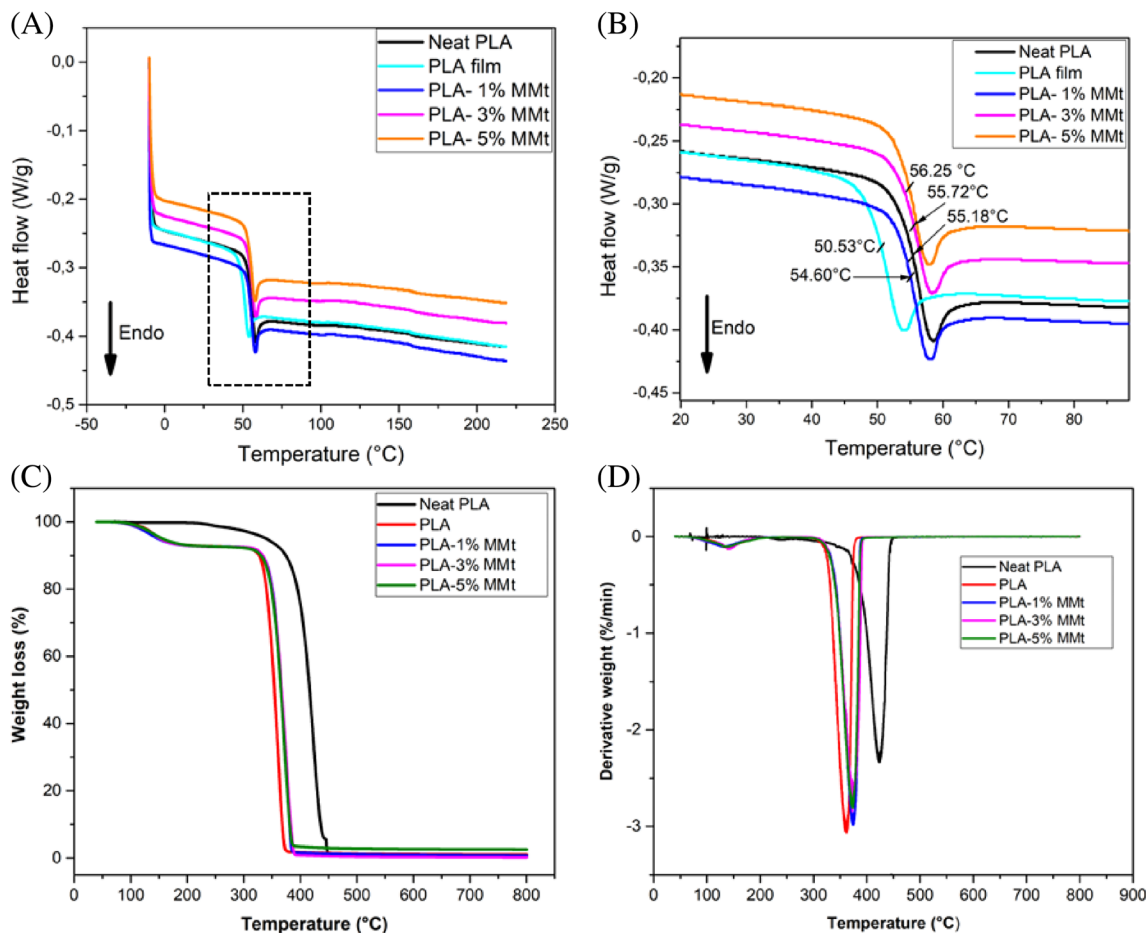


FIGURE 8 (A) Differential scanning calorimetry thermograms of neat poly(lactic acid) (PLA) granules, films formed from aqueous PLA and PLA-MMt (1, 3, and 5 wt%) emulsions prepared using SO/Tw80 (20:80) formulation. (B) Zoom on the glass transition zone of all samples. (C) Thermogravimetric analysis (TGA) results and (D) the derivative curves of TGA analysis (DTG). MMt, modified montmorillonite.

weights, and so on.⁵⁶ The second area, between 250 and 420°C where more than 90% of the sample's weights were lost due to depolymerization and full decomposition of PLA. During the thermal degradation of PLA, several reactions occur, such as inter and intramolecular exchange of ester groups leading to the formation of cyclic oligomers and lactides, random main chains scissions, hydrolysis, and oxidative degradation.⁵⁷ Neat PLA pellets exhibited high thermal stability with the initial degradation temperature (T_i) recorded at 286°C, however, this temperature is lower than the T_i exhibited by semi-crystalline PLA, which occurs mostly at 320°C depending on the polymer grade. This result was expected since the PLA used in our study is amorphous with low molecular weight, it is well established that amorphous structures with random polymer chains arrangements provide an open molecular structure, which tolerates oxygen penetration and thus thermal degradation by oxidative reaction occurs.^{55,58} PLA film sample prepared from the PLA-emulsion, where the T_i has been reduced to 197°C,

same reduction behavior has been observed for samples containing surface MMt (1, 3, and 5 wt%) with a small increase when compared with unfilled PLA film as intended for the organoclay nanofillers used generally as to improve the thermostability of polymeric matrices, like for semicrystalline PLA,⁵⁹ poly(ϵ -caprolactone),⁶⁰ and nylon-6.⁶¹ The phyllosilicate organoclay increase the tortuous pathway of the polymer matrix and thus delay the diffusion of the combustion by-products,⁶² the recorded T_i were 256, 277, and 285°C for PLA containing 1, 3, and 5 wt% of MMt, respectively. Moreover, from the derivative thermogram analysis (DTG) presented in Figure 8D we can observe one degradation peak for all samples representing the maximum degradation temperature (T_{max}) at which the thermal degradation rate of the polymer reaches its maximum. The T_{max} has been reduced from 410°C for neat PLA to 289°C for PLA film, however a small increase was observed for the nanocomposites (PLA-MMt (1, 3, and 5 wt%)) to 362, 373, and 374°C, respectively. The char residue at the final

TABLE 4 Thermal properties obtained by thermogravimetric/derivative thermogravimetric analyses.

Samples	T_i (°C)	T_{max} (°C)	Weight loss at T_{max} (%)	Char residue (%) at 800 (°C)
Neat PLA	286	410	99.08	0.30
PLA	197	289	98.39	0.88
PLA-1% MMt	256	362	98.27	1.20
PLA-3% MMt	277	373	98.06	2.13
PLA-5% MMt	285	374	96.44	3.11

Abbreviations: MMt, modified montmorillonite; PLA, polylactic acid.

temperature (800°C) for Neat PLA was 0.30% and increased in the case of PLA film to 0.88% due to the presence of surfactants, this increase was more important in the case of the nanocomposites up to 3.11%, attributed to the nanofillers and increases by increasing the amount of MMt from 1 to 5 wt%, all the data from TGA/DTG analyses are resumed in Table 4.

Overall, the TGA/DTG results are in accordance with DSC results in which the surfactants used to prepare the aqueous dispersions acted like plasticizers and thus T_g , T_i , and T_{max} have been reduced compared with the same characteristic temperatures of untreated PLA pellets. This behavior can be explained by the disorganization at the macromolecular level caused by the surfactants generating more freedom and mobility for PLA chains, same results have been reported by Calambas Pulgarin et al.⁶³ and Fonseca-García et al.,⁶⁴ also since we used a water-based process to prepare PLA emulsions, the retained water favored and accelerated PLA decomposition by hydrolysis.⁶⁵ However, adding small amounts of MMt have led to a recovery in the thermal stability by confining the mobility of PLA chains which is an inverse effect to surfactant effect and moreover due to the generated tortuous pathway in PLA matrix and its fire-retardant properties, yet it is important to mention that in our case the surfactant effect was more dominant than the organoclay effect.^{9,66}

4.3 | Rheology measurements

The data show a similar rheological behavior for all tested samples as presented in Figure 9A. A non-Newtonian behavior with a shear-thinning flow was recorded for all tested samples, the recorded apparent viscosities (η) decreased by increasing shear rate ($\dot{\gamma}$) to achieve a constant value at high shear rates (630 s⁻¹). Thickened emulsions were much more viscous than the aqueous PLA emulsions. To better observe the data, Figure 9B–E demonstrate a binary comparison between thickened emulsions and aqueous emulsions without xanthan gum. These results were expected since xanthan

gum in contact with water creates a three-dimensional network in form of weak microgel structure, moreover xanthan gum presents a second structure consisting on a five-fold helical structure combined with its high molecular weight, which were the reasons why thickened emulsions showed high viscosities⁶⁷ and in our case, it is more likely that the suspended PLA nanoparticles acted like fillers and reinforced the gel structure which contributed to the increase in the overall viscosity of the thickened samples.⁶⁸

On the other hand, in the case of the aqueous PLA emulsions containing MMt at different weights 1, 3, and 5 wt%, results in Figure 10A indicated that samples containing MMt exhibit higher viscoelastic than neat PLA aqueous emulsion. The dilatant behavior presented in Figure 10B may be attributed to the elastic response from the interfaces during the particle's collision.⁶⁹ Organically modified clays are used to control the flow of organic systems like cosmetic creams, paints, and so on.⁷⁰ To the best of our knowledge, rheological studies of polymer/organoclay water-based emulsions are not sufficiently studied. However, the use of natural hydrophilic clays as rheological additives for diverse aqueous fluids is well known, such as montmorillonite,⁷¹ sepiolite,⁷² and palygorskite.⁷³ This increase in viscosity is attributed to the strong interactions between the clay layers generating a network structure. The formation of this structure through a gelation process is mainly due to a specific linkage between the positive edge and the negative surface of the parallel plates of clay (house of cards structure) or between the edges (ribbons structure).⁷⁴ However, it is a different mechanism for the organically modified clay. The most application that reported the use of organoclays as rheology additives is the oil-based drilling fluids, where the process is well defined. As reported by Zhuang et al.⁷⁴ and Silva et al.,⁷⁵ excellent rheological properties were found when organoclay were added to the oil-based drilling fluids. These results were attributed to the swelling ability of organoclays when dispersed in the oil phase and the increase of the basal spacing creating exfoliated structure which promotes linkages like edge-surface and edge-edge types between the organoclays layers resulting in the

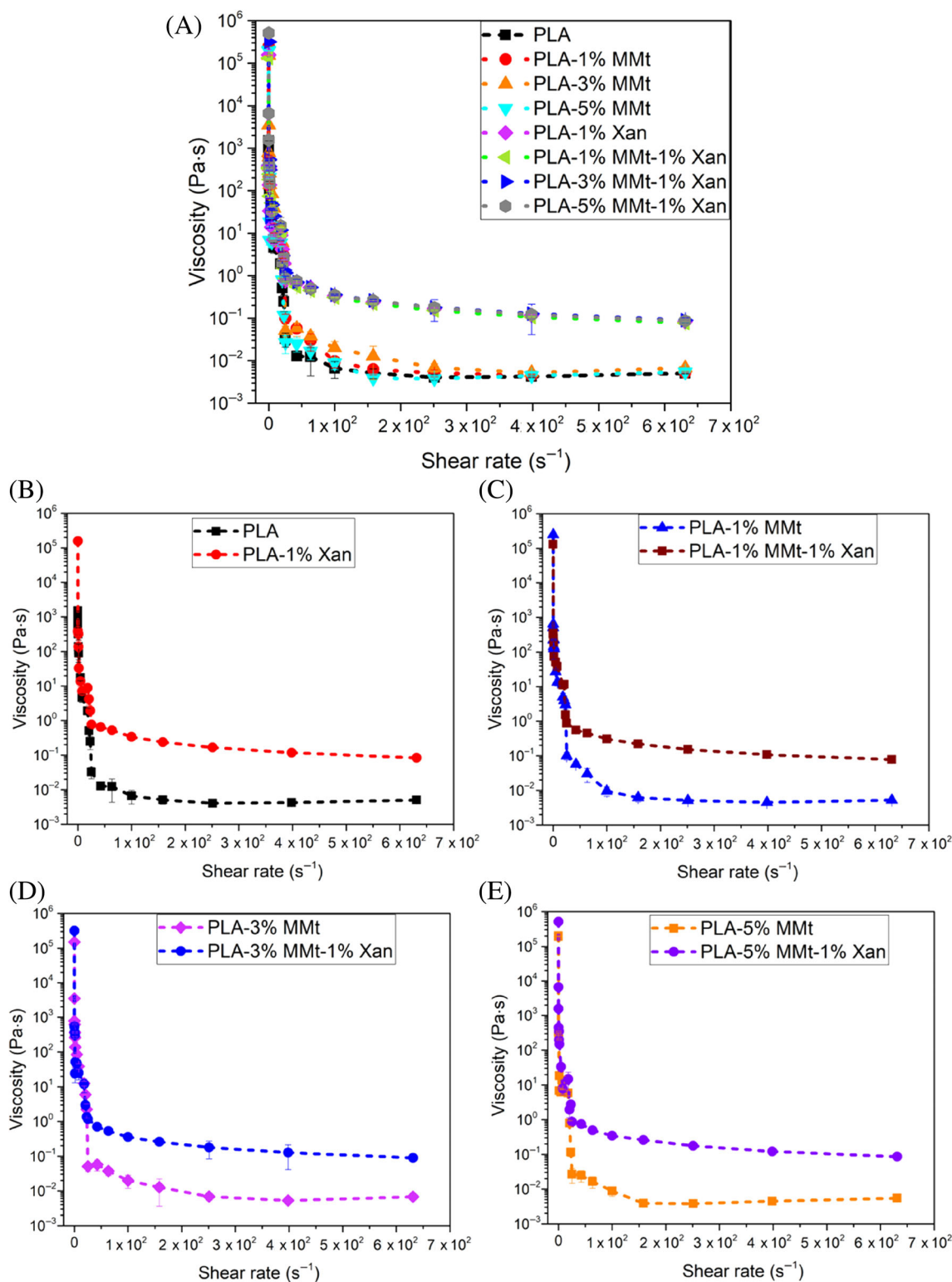


FIGURE 9 Viscosity versus shear rate plots of (A) all samples aqueous and thickened poly(lactic acid) (PLA) emulsions, and binary comparison between thickened and aqueous emulsions (B) PLA and PLA thickened by 1 wt% xanthan gum (Xan) (C) PLA-1 wt% modified montmorillonite (MMt) and PLA-1 wt% MMt thickened by 1 wt% Xan (D) PLA-3 wt% MMt and PLA-3 wt% MMt thickened by 1 wt% Xan and (E) PLA-5 wt% MMt and PLA-5 wt% MMt thickened by 1 wt% Xan.

formation of a gel as reported by Fu et al.⁷⁰ on polystyrene containing organically MMt. In our work, these findings explain the structure modifications of MMt dispersed in

ethyl acetate to prepare the organic phase. However, after the solvent evaporates, the PLA droplets containing MMt hardens and therefore the expansion and the swelling of

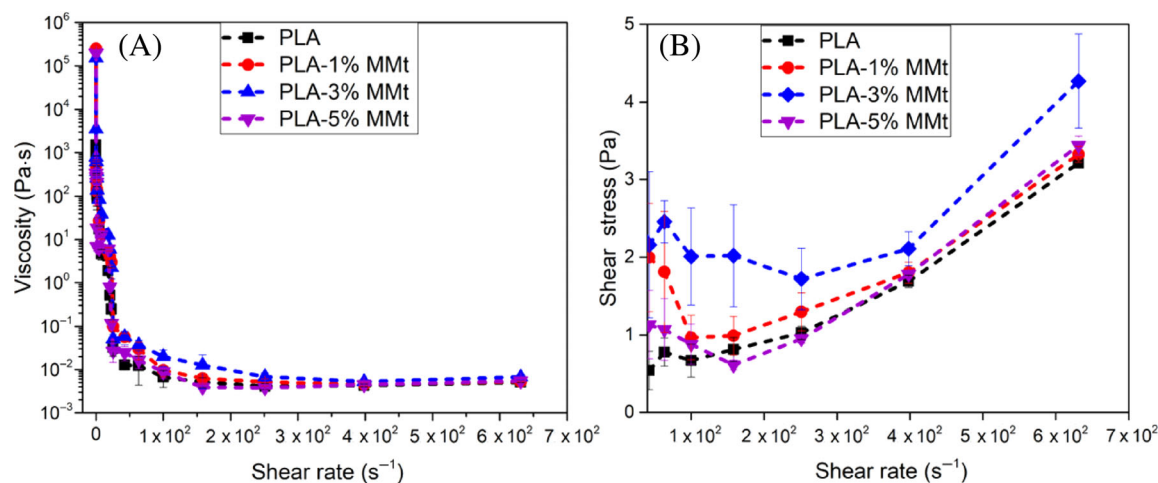


FIGURE 10 (A) Viscosity versus shear rate plots and (B) shear stress versus shear rate plots of poly(lactic acid) (PLA) aqueous emulsions containing 1, 3, and 5 wt% of modified montmorillonite (MMt).

the MMt particles were limited and leaving the interactions between the clay lamellae at the surface level of the PLA particles, thus the increase in the viscosity was not significant.

5 | CONCLUSION

Aqueous PLA emulsions filled with surface MMt as a nanofiller were successfully produced using a simple emulsification-solvent diffusion method with the use of less harmful emulsifiers and solvent. To apply the chosen formulations as coatings for paper, xanthan gum was used as a food grade thickening agent. The developed emulsions showed high thermodynamic stability (up to 5 months at $23 \pm 1^\circ\text{C}$) due to the steric and electrostatic stabilization mechanisms with a film formation ability fulfilling the criteria for a thermoscelable coating's applications. The present work represents a successful use of the simple method emulsification-solvent evaporation to prepare biobased nanocomposites aqueous emulsions as a replacement to the mini-emulsions and the conventional polymerization emulsion method. The good promising results obtained in this work confirmed that aqueous biobased barrier coatings developed using low-toxic solvent and food grade emulsifiers and thickening agent can be produced and applied as a substitute to the commercial nonbiodegradable barrier coatings for packaging paper.

ACKNOWLEDGMENTS

The authors would also like to acknowledge the participation of students and technicians in the current work of Dr. Vu Nhu Nang (UQTR, Canada), (Innofibre, Cégep de

Trois-Rivières, Canada), and Kéziah Milette, Céline Leduc, Isabelle Boulan (I2E3, UQTR, Canada).

DATA AVAILABILITY STATEMENT

Research data are not shared.

ORCID

Phuong Nguyen-Tri  <https://orcid.org/0000-0001-6578-5716>

REFERENCES

- Amin KF, Asrafuzzaman, Nahin AM, Hoque ME. Chapter 10. Polymer nanocomposites for adhesives and coatings. In: Hoque ME, Ramar K, Sharif A, eds. *Advanced Polymer Nanocomposites: Science, Technology and Applications*. Woodhead Publishing; 2022:253-265. doi:10.1016/B978-0-12-824492-0.00014-3
- Pielichowski K, Pielichowska K. Chapter 11. Polymer nanocomposites. In: Vyazovkin S, Koga N, Schick C, eds. *Handbook of Thermal Analysis and Calorimetry*. 2nd ed. Elsevier Science B.V; 2018:431-485. doi:10.1016/B978-0-444-64062-8.00003-6
- Tofighty MA, Mohammadi T. Chapter 5. Carbon nanotubes-polymer nanocomposite membranes for pervaporation. In: Thomas S, George SC, Jose T, eds. *Polymer Nanocomposite Membranes for Pervaporation A Volume in Micro and Nano Technologies*. Elsevier Inc; 2020:105-133. doi:10.1016/B978-0-12-816785-4.00005-7
- Swetha TA, Ananthi V, Bora A, et al. A review on biodegradable poly(lactic acid) (PLA) production from fermentative food waste—its applications and degradation. *Int J Biol Macromol*. 2023;234:123703. doi:10.1016/j.ijbiomac.2023.123703
- Picard E, Espuche E, Fulchiron R. Effect of an organo-modified montmorillonite on PLA crystallization and gas barrier properties. *Appl Clay Sci*. 2011;53:58-65. doi:10.1016/j.clay.2011.04.023
- Ahmed J, Varshney SK. Poly(lactides)—chemistry, properties and green packaging technology: a review. *Int J Food Prop*. 2011;14:37-58. doi:10.1080/10942910903125284

7. Murariu M, Dubois P. PLA composites: from production to properties. *Adv Drug Deliv Rev.* 2016;107:17-46. doi:10.1016/j.addr.2016.04.003
8. Chow WS, Teoh EL, Karger-Kocsis J. Flame retarded poly(lactic acid): a review. *EXPRESS Polym Lett.* 2018;12:396-417. doi:10.3144/expresspolymlett.2018.34
9. Yilmaz O, Cheaburu CN, Durraccio D, Gulumser G, Vasile C. Preparation of stable acrylate/montmorillonite nanocomposite latex via in situ batch emulsion polymerization: effect of clay types. *Appl Clay Sci.* 2010;49:288-297. doi:10.1016/j.clay.2010.06.007
10. Leszczyńska A, Njuguna J, Pielichowski K, Banerjee JR. Polymer/montmorillonite nanocomposites with improved thermal properties: part I. Factors influencing thermal stability and mechanisms of thermal stability improvement. *Thermochim Acta.* 2007;453:75-96. doi:10.1016/j.tca.2006.11.002
11. Purnama P, Jung Y, Kim SH. An advanced class of bio-hybrid materials: bionanocomposites of inorganic clays and organic stereo complex poly(lactides). *Macromol Mater Eng.* 2013;298:263-269. doi:10.1002/mame.201200073
12. Fambri L, Dorigato A, Pegorett A. Role of surface-treated silica nanoparticles on the thermo-mechanical behavior of poly(lactide). *Appl Sci.* 2020;10:6731. doi:10.3390/app10196731
13. Wu D, Wu L, Wu L, Xu B, Zhang Y, Zhang M. Nonisothermal cold crystallization behavior and kinetics of poly(lactide)/clay nanocomposites. *J Polym Sci B.* 2007;45:1100-1113. doi:10.1002/polb.21154
14. Othman SH, Ling HN, Talib RA, Naim MN, Risyon NP, Saifullah M. PLA/MMT and PLA/halloysite bio-nanocomposite films: mechanical, barrier, and transparency. *J Nano Res.* 2019;59:77-93. doi:10.4028/www.scientific.net/jnanor.59.77
15. Chang Y, Guo K, Guo KL, et al. Ploy(lactic acid)/organo-modified montmorillonite nanocomposites for improved eletret properties. *J Electrostat.* 2016;80:17-21. doi:10.1016/j.elstat.2016.01.001
16. Castillo-Pérez R, Hernández-Vargas ML, Flores-Cedillo O, Campillo-Illanes BF. Effect on thermo-mechanical properties by in-situ emulsion polymerization of polymer/clay nanocomposites. *Polym Compos.* 2017;40:263-276. doi:10.1002/pc.24640
17. Wang X, Su Q, Shan J, Zheng J. The effect of clay modification on the mechanical properties of poly(methyl methacrylate)/organomodified montmorillonite nanocomposites prepared by in situ suspension polymerization. *Polym Compos.* 2014;37:1705-1714. doi:10.1002/pc.23343
18. Bagheri S, Kalantari M, Fozooni S, Rafsanjani HH. Synthesis of organic-inorganic hybrid nanocomposites based on the acrylate monomers and investigation of scratch resistance of these nanocomposites. *Polym Compos.* 2020;41:142-160. doi:10.1002/pc.25353
19. Kartaloğlu N, Delibaş A. Laponite/magnetite nanoparticles including waterborne latexes and effect of conditions for stable composite latexes. *Polym Compos.* 2023;45:1508-1523. doi:10.1002/pc.27870
20. Mičušík M, Bonnefond A, Reyes Y, et al. Morphology of polymer/clay latex particles synthesized by miniemulsion polymerization: modeling and experimental results. *Macromol React Eng.* 2010;4:432-444. doi:10.1002/mren.200900084
21. Chenni A, Eesae M, Stuppa C, et al. Water vapor and air barrier performance of sustainable paper coatings based on PLA and xanthan gum. *Mater Today Commun.* 2023;36:106626. doi:10.1016/j.mtcomm.2023.106626
22. Belletti G, Buoso S, Ricci L, et al. Preparations of poly(lactic acid) dispersions in water for coating applications. *Polymers.* 2021;13:2767. doi:10.3390/polym13162767
23. Given PS. Encapsulation of flavors in emulsions for beverages. *Curr Opin Colloid Interface Sci.* 2009;14:43-47. doi:10.1016/j.cocis.2008.01.007
24. Zhang R, McClements DJ. Enhancing nutraceutical bioavailability by controlling the composition and structure of gastrointestinal contents: emulsion-based delivery and excipient systems. *Food Struct.* 2016;10:21-36. doi:10.1016/j.foostr.2016.07.006
25. Tadros T, Izquierdo P, Esquena J, Solans C. Formation and stability of nano-emulsions. *Adv Chem Phys.* 2004;108-109:303-308. doi:10.1016/j.cis.2003.10.023
26. Zhang S, Zhang Q, Shang J, Mao Z-s, Yang C. Measurement methods of particle size distribution in emulsion polymerization. *Chin J Chem Eng.* 2021;39:1-15. doi:10.1016/j.cjche.2021.03.007
27. Sun Q, Deng Y, Wang ZL. Synthesis and characterization of polystyrene-encapsulated laponite composites via miniemulsion polymerization. *Macromol Mater Eng.* 2004;289:288-295. doi:10.1002/mame.200300219
28. Feiz S, Navarchian AH. Emulsion polymerization of styrene: simulation the effects of mixed ionic and non-ionic surfactant system in the presence of coagulation. *Chem Eng Sci.* 2012;69:431-439. doi:10.1016/j.ces.2011.10.063
29. Wu Z, Wu J, Zhang R, Yuan S, Lu Q, Yu Y. Colloid properties of hydrophobic modified alginate: surface tension, ζ -potential, viscosity and emulsification. *Carbohydr Polym.* 2018;181:56-62. doi:10.1016/j.carbpol.2017.10.052
30. Astete CE, Sabliov CM, Watanabe F, Biris A. Ca²⁺ cross-linked alginic acid nanoparticles for solubilization of lipophilic natural colorants. *J Agric Food Chem.* 2009;57:7505-7512. doi:10.1021/jf900563a
31. Ruiz E, Orozco VH, Hoyos LM, Giraldo LF. Study of sonication parameters on PLA nanoparticles preparation by simple emulsion-evaporation solvent technique. *Eur Polym J.* 2022;173:111307. doi:10.1016/j.eurpolymj.2022.111307
32. Mirzataheri M, Mahdavian AR, Atai M. Nanocomposite particles with core-shell morphology IV: an efficient approach to the encapsulation of Cloisite 30B by poly(styrene-co-butyl acrylate) and preparation of its nanocomposite latex via miniemulsion polymerization. *Coll Polym Sci.* 2009;287:725-732. doi:10.1007/s00396-009-2020-5
33. Wu Y, Zhang J, Zhao H. Functional colloidal particles stabilized by layered silicate with hydrophilic face and hydrophobic polymer brushes. *J Polym Sci Part A: Polym Chem.* 2009;47:1535-1543. doi:10.1002/pola.23256
34. Mairdarker SN, Bongers P, Henson MA. Predicting the effects of surfactant coverage on drop size distributions of homogenized emulsions. *Chem Eng Sci.* 2013;89:102-114. doi:10.1016/j.ces.2012.12.001
35. Riebesehl BU. Chapter 29. Drug delivery with organic solvents or colloidal dispersed systems. In: Wermuth CG, Aldous D, Raboisson P, Rognan D, eds. *The Practice of Medicinal Chemistry.* 4th ed. Academic Press; 2015:699-722. doi:10.1016/B978-0-12-417205-0.00029-8
36. Panchal B, Truong T, Prakash S, Bansal N, Bhandari B. Influence of emulsifiers and dairy ingredients on manufacturing,

- microstructure, and physical properties of butter. *Foods*. 2021; 10:1140. doi:10.3390/foods10051140
37. Wu S, Wang G, Lu Z, et al. Effects of glycerol monostearate and Tween 80 on the physical properties and stability of recombined low-fat dairy cream. *Dairy Sci Technol*. 2016;96:377-390. doi:10.1007/s13594-015-0274-x
 38. Roldan-Cruz C, Vernon-Carter EJ, Alvarez-Ramirez J. Assessing the stability of Tween 80-based O/W emulsions with cyclic voltammetry and electrical impedance spectroscopy. *Colloids Surf A Physicochem Eng Asp*. 2016;511:145-152. doi:10.1016/j.colsurfa.2016.09.074
 39. Tong Z, Deng Y. Synthesis of water-based polystyrene–nanoclay composite suspension via miniemulsion polymerization. *Ind Eng Chem Res*. 2006;45:2641-2645. doi:10.1021/ie0509600
 40. Cheng D, Ariafar S, Sheibat-Othman N, Pohn J, McKenna TFL. Particle coagulation of emulsion polymers: a review of experimental and modelling studies. *Polym Rev*. 2018;58:717-759. doi:10.1080/15583724.2017.1405979
 41. Diaconu G, Paulis M, Leiza JR. High solids content waterborne acrylic/montmorillonite nanocomposites by miniemulsion polymerization. *Macromol React Eng*. 2008a;2:80-89. doi:10.1002/mren.200700039
 42. Tabaniag JSU, Abad MQD, Morcelos CJR, Geraldino GVB, Alvarado JLM, Lopez ECR. Stabilization of oil/water emulsions using soybean lecithin as a biobased surfactant for enhanced oil recovery. *J Eng Appl Sci*. 2023;70:154. doi:10.1186/s44147-023-00322-5
 43. Ortega-Toro R, Jiménez A, Talens P, Chiralt A. Effect of the incorporation of surfactants on the physical properties of corn starch films. *Food Hydrocoll*. 2014;38:66-75. doi:10.1016/j.foodhyd.2013.11.011
 44. Zhou CH, Zhang D, Tong DS, Wu LM, Yu WH, Ismadji S. Paperlike composites of cellulose acetate–organo-montmorillonite for removal of hazardous anionic dye in water. *J Chem Eng*. 2012; 209:223-234. doi:10.1016/j.ccej.2012.07.107
 45. Yu WH, Zhu TT, Tong DS, Wang M, Wu QQ, Zhou CH. Preparation of organo-montmorillonites and the relationship between microstructure and swellability. *Clays Clay Miner*. 2017;65:417-430. doi:10.1346/CCMN.2017.064068
 46. Gardi I, Mishael YG. Designing a regenerable stimuli-responsive grafted polymer-clay sorbent for filtration of water pollutants. *Sci Technol Adv Mater*. 2018;19:588-598. doi:10.1080/14686996.2018.1499381
 47. Zhou CH, Li CJ, Gates WP, Zhu TT, Yu WH. Co-intercalation of organic cations/amide molecules into montmorillonite with tunable hydrophobicity and swellability. *Appl Clay Sci*. 2019; 179:105157. doi:10.1016/j.clay.2019.105157
 48. As'habi L, Jafari SH, Khonakdar HA, Kretschmar B, Wagenknecht U, Heinrich G. Effect of clay type and polymer matrix on microstructure and tensile properties of PLA-/LLDPE/clay nanocomposites. *J Appl Polym Sci*. 2013;130:749-758. doi:10.1002/APP.39209
 49. Zhu TT, Zhou CH, Kabwe FB, Wu QQ, Li CS, Zhang JR. Exfoliation of montmorillonite and related properties of clay/polymer nanocomposites. *Appl Clay Sci*. 2019;169:48-66. doi:10.1016/j.clay.2018.12.006
 50. Mohamad N, Mazlan MM, Tawakkal ISMA, et al. Development of active agents filled polylactic acid films for food packaging application. *Int J Biol Macromol*. 2020;163:1451-1457. doi:10.1016/j.ijbiomac.2020.07.209
 51. Villegas C, Arrieta MP, Rojas A, et al. PLA/organoclay bionanocomposites impregnated with thymol and cinnamaldehyde by supercritical impregnation for active and sustainable food packaging. *Compos B Eng*. 2019;176:107336. doi:10.1016/j.compositesb.2019.107336
 52. Connolly M, Zhang Y, Brown DM, et al. Novel polylactic acid (PLA)-organoclay nanocomposite bio-packaging for the cosmetic industry; migration studies and in vitro assessment of the dermal toxicity of migration extracts. *Polym Degrad Stab*. 2019; 168:108938. doi:10.1016/j.polymdegradstab.2019.108938
 53. Negrete-Herrera N, Putaux J-L, David L, De Haas F, Bourgeat-Lami E. Polymer/laponite composite latexes: particle morphology, film microstructure, and properties. *Macromol Rapid Commun*. 2007;28:1567-1573. doi:10.1002/marc.200700212
 54. Ozkoc G, Kemaloglu S. Morphology, biodegradability, mechanical, and thermal properties of nanocomposite films based on PLA and plasticized PLA. *J Appl Polym Sci*. 2009;114:2481-2487. doi:10.1002/app.30772
 55. Jamshidian M, Tehrani EA, Imran M, Jacquot M, Desobry S. Poly-lactic acid: production, applications, nanocomposites, and release studies. *Compr Rev Food Sci Food Saf*. 2010;9:552-571. doi:10.1111/j.1541-4337.2010.00126.x
 56. Zhou Q, Xanthos M. Nanosize and microsize clay effects on the kinetics of the thermal degradation of polylactides. *Polym Degrad Stab*. 2009;94:327-338. doi:10.1016/j.polymdegradstab.2008.12.009
 57. Gao H, Hu S, Su F, Zhang J, Tan G. Mechanical, thermal, and biodegradability properties of PLA/modified starch blends. *Polym Compos*. 2011;32:2093-2100. doi:10.1002/pc.21241
 58. Wong AC-Y, Lam F. Study of selected thermal characteristics of polypropylene/polyethylene binary blends using DSC and TGA. *Polym Test*. 2002;21:691-696. doi:10.1016/S0142-9418(01)00144-1
 59. Chenni A, Djedjelli H, Boukerrou A, Martinez Vega JJ, Grohens Y, Saulnier B. Ternary melt blend based on poly (lactic acid)/chitosan and cloisite 30B: a study of microstructural, thermo-mechanical and barrier properties. *Mater Test*. 2018;60: 825-832. doi:10.3139/120.111219
 60. Pantoustier N, Lepoittevin B, Alexandre M, et al. Biodegradable polyester layered silicate nanocomposites based on poly (ϵ -caprolactone). *Polym Eng Sci*. 2004;42:1928-1937. doi:10.1002/pen.11085
 61. Kumaresan S, Rokade DS, Marathe YN, et al. Synthesis and characterization of nylon 6 polymer nanocomposite using organically modified Indian bentonite. *SN Appl Sci*. 2020;2: 1412. doi:10.1007/s42452-020-2579-5
 62. Wei P, Bocchini S, Camino G. Nanocomposites combustion peculiarities. A case history: polylactide-clays. *Eur Polym J*. 2013;49:932-939. doi:10.1016/j.eurpolymj.2012.11.010
 63. Calambas Pulgarin HL, Caicedo C, Florez Lopez E. Effect of surfactant content on rheological, thermal, morphological and surface properties of thermoplastic starch (TPS) and polylactic acid (PLA) blends. *Heliyon*. 2022;8:e10833. doi:10.1016/j.heliyon.2022.e10833
 64. Fonseca-García A, Osorio BH, Aguirre-Loredo RY, Calambas HL, Caicedo C. Miscibility study of thermoplastic starch/polylactic acid blends: thermal and superficial

- properties. *Carbohydr Polym.* 2022;293:119744. doi:[10.1016/j.carbpol.2022.119744](https://doi.org/10.1016/j.carbpol.2022.119744)
65. Morawa Eblagon STK, Fernando R, Pereira FMM, Figueiredo JL. Towards controlled degradation of poly(lactic) acid in technical applications. *J Carbon Res.* 2021;7:42. doi:[10.3390/c7020042](https://doi.org/10.3390/c7020042)
66. Sermsantiwanit K, Phattananurudee S. Preparation of bio-based nanocomposite emulsions: effect of clay type. *Prog Org Coat.* 2012;74:660-666. doi:[10.1016/j.porgcoat.2011.09.033](https://doi.org/10.1016/j.porgcoat.2011.09.033)
67. Moffat J, Morris VJ, Al-Assaf S, Gunning AP. Visualisation of xanthan conformation by atomic force microscopy. *Carbohydr Polym.* 2016;148:380-389. doi:[10.1016/j.carbpol.2016.04.078](https://doi.org/10.1016/j.carbpol.2016.04.078)
68. Krstonošić V, Dokić L, Nikolić I, Milanović M. Influence of xanthan gum on oil-in-water emulsion characteristics stabilized by OSA starch. *Food Hydrocoll.* 2015;45:9-17. doi:[10.1016/j.foodhyd.2014.10.024](https://doi.org/10.1016/j.foodhyd.2014.10.024)
69. Kumar N, Mandal A. Surfactant stabilized oil-in-water nanoe-mulsion: stability, interfacial tension, and rheology study for enhanced oil recovery application. *Energy Fuel.* 2018;32:6452-6466. doi:[10.1021/acs.energyfuels.8b00043](https://doi.org/10.1021/acs.energyfuels.8b00043)
70. Qi J, Yu J, Shah KJ, Shah DD, Yo Z. Applicability of clay/organic clay to environmental pollutants: green way—an overview. *Appl Sci.* 2023;13:9395. doi:[10.3390/app13169395](https://doi.org/10.3390/app13169395)
71. Abdo J, Haneef MD. Clay nanoparticles modified drilling fluids for drilling of deep hydrocarbon wells. *Appl Clay Sci.* 2013;86:76-82. doi:[10.1016/j.clay.2013.10.017](https://doi.org/10.1016/j.clay.2013.10.017)
72. Al-Malki N, Pourafshary P, Al-Hadrami H, Abdo J. Controlling bentonite-based drilling mud properties using sepiolite nanoparticles. *Pet Explor Dev.* 2016;43:717-723. doi:[10.1016/S1876-3804\(16\)30084-2](https://doi.org/10.1016/S1876-3804(16)30084-2)
73. Santanna VC, Silva SL, Silva RP, Castro Dantas TN. Use of palygorskite as a viscosity enhancer in salted water-based muds: effect of concentration of palygorskite and salt. *Clay Miner.* 2020;55:48-52. doi:[10.1180/clm.2020.7](https://doi.org/10.1180/clm.2020.7)
74. Zhuang G, Zhang Z, Jaber M. Organoclays used as colloidal and rheological additives in oil-based drilling fluids: an overview. *Appl Clay Sci.* 2019;177:63-81. doi:[10.1016/j.clay.2019.05.006](https://doi.org/10.1016/j.clay.2019.05.006)
75. Silva IA, Sousa FKA, Menezes RR, Neves GA, Santana LNL, Ferreira HC. Modification of bentonites with nonionic surfactants for use in organic-based drilling fluids. *Appl Clay Sci.* 2014;95:371-377. doi:[10.1016/j.clay.2014.04.021](https://doi.org/10.1016/j.clay.2014.04.021)

How to cite this article: Abdenour C, Nguyen-Tri P, Chabot B, et al. New stable waterborne amorphous polylactic acid/organoclay nanocomposites prepared using emulsification solvent evaporation method. *Polym Compos.* 2024; 1-20. doi:[10.1002/pc.28681](https://doi.org/10.1002/pc.28681)